Regular Article

PHYSICAL CHEMISTRY RESEARCH
Published by the
Iranian Chemical Society
www.physchemres.org
info@physchemres.org

Phys. Chem. Res., Vol. 9, No. 4, 605-621, December 2021
DOI: 10.22036/PCR.2021.274568.1889

Comparative Study of Adsorption of Safranin o by TiO_2/Activated Carbon and Chitosan/TiO_2/Activated Carbon Adsorbents

S. Sharafinia[a], A. Farrokhnia[a,*] and E. Ghasemian Lemraski[b]

[a]*Department of Chemistry, Faculty of Science, Shahid Chamran University of Ahvaz, Ahvaz, Iran*
[b]*Department of Chemistry, Faculty of Science, Ilam University, Ilam, Iran*

(Received 22 February 2021, Accepted 8 July 2021)

This research is a comparative study of the surface chemistry and adsorptive characteristics of titanium dioxide nanoparticles on activated carbon (Ac/TiO_2) and chitosan loaded on activated carbon (Ac/TiO_2/Ch). For the first time, a three-fold composite of activated carbon was prepared from Persian mesquite seeds, chitosan, and nanoparticles of titanium dioxide as an effective adsorbent for removal of safranin o. X-ray Diffraction (XRD), scanning electron microscope (SEM), BET analysis and thermogravimetric analysis (TGA) have been used to determine and confirm the physicochemical variations during the preparation and modification of activated carbon on both adsorbents. The results of XRD, SEM and TGA showed that the essential changes happened in porosity of the surface after the modification process. The Ac/TiO_2 and Ac/TiO_2/Ch adsorbents have been used to remove the safranin o, a cationic azo dye, from an aqueous solution. The experimental data at different conditions were correlated with some famous kinetic and isotherm models. Extrapolated data showed that the dye adsorption on the Ac/TiO_2 and Ac/TiO_2/Ch follows the pseudo-second-order kinetic model. High efficiency and sufficient adsorption capacity of Ac/TiO_2/Ch for safranin o removal makes it a good candidate for water filtration.

Keywords: Activated carbon, TiO_2NP_S Chitosan, Removal of Safranin o

INTRODUCTION

Water pollution occurs when toxic compounds enter the water, change the water quality, and make it harmful to the environment or humans. Among different industrial compounds, dye is widely used in the textile, leather, food, plastic, and paper industries [1]. Approximately 4-5% of azo dyes can potentially form dangerous compounds to human health and the environment. Specifically, many researchers reported the relation between these dyes and some cancers [2-5].

Recently, biological, chemical and physical techniques have been used for dye removal from wastewater. Adsorption is one of the essential physical methods for removing pollutions from wastewaters [6]. Several surface-active materials such as natural compounds, polymers and different forms of metal oxides have been used to remove pollutants from the wastewater.

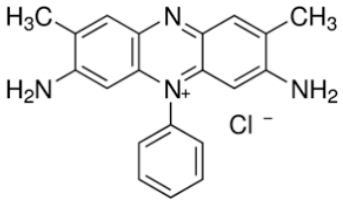

Fig. 1. Chemical structure of safranin o.

In the present research, we focus on the study of adsorption of safranin o (see Fig. 1 and Table 1) on activated carbon modified with TiO_2 and chitosan. Activated carbon prepared from mosquito grain by chemical method. Activated carbon with a high surface area is a good candidate for adsorption of certain pollutants such as

*Corresponding author. E-mail: farrokhnia@scu.ac.ir

Table 1. Some Properties of Safranin o Dye

Name	C. I. Name	Colour index number	Empirical formula	Molecular weight	λ_{max}
Safranin o	Basic red 2	C.I. 50240	$C_{20}H_{19}N_4Cl$	350.84	518 nm

organic and inorganic substances [7].

Surface modification and functionalization of activated carbon with the adsorbent molecules are interested subjects to scholars [8]. Titanium dioxide nanoparticles (TiO_2NP_S) have been widely used as pigment, adsorbent, catalyst support, filter, coating, photoconductor and dielectric material [9]. Also, chitosan as a biopolymer has been used to adsorb pollutants such as dyes, proteins, metal ions, *etc.* [10]. Evaluation of the performance of Ac/TiO_2NP_s and Ac/TiO_2/Ch for dye removal is the main purpose of this work. The novelty of this study firstly is about the activated carbon, which is prepared from Persian mesquite seeds. Secondly, coating the prepared activated carbon with materials of biological origin is a new method for modifying and developing the properties of activated carbon. With this modification, much smaller amounts of activated carbon will be required in the adsorption process, and the removal process will become a cost-effective and environmentally friendly process. One of the biological sources of adsorbent is chitosan, a type of chitin acetylation (a natural polymer found in several sources such as crustaceans and fungous cell walls) that has many applications in biochemistry, pharmacy, medicine, agriculture and wastewater treatment. The amine and hydroxyl functional groups of chitosan can adsorb dyes through several mechanisms, including chemical interactions and electrostatic interactions (*e.g.*, ion-exchange or ion pair formation). The type of interaction depends on the form of dyes, and the pH of the solution. Chitosan and its derivatives such as cross-linked chitosan, chitosan granules and chitosan composites have been studied as adsorbents for the removal of dyes from aqueous solutions. Also, in the hybrid form, activated carbon (prepared from mesquite seeds) is new, and its hybrid has not been synthesized with other materials so far. In the present work, titanium dioxide nanoparticles (TiO_2NP_S) and chitosan (Ch) were loaded on activated carbon (Ac) to enhance the absorptivity of activated carbon and then these adsorbents characterized by using methods such as TGA, SEM and XRD. These techniques have also been used to determine the essential changes during the preparation of adsorbents. For studying the surface area of prepared adsorbents, BET surface area, pore size, and pore volume distribution were measured and estimated using nitrogen gas adsorption at 77 K. The adsorbents used in this work have excellent performance for adsorption of safranin dye. Five effective parameters such as pH, initial concentration, time, adsorbent dose and temperature are optimized and the outcomes are compared. Consequently, the obtained experimental data have been used to determining surface adsorption capacity, kinetic and thermodynamic parameters.

EXPERIMENTAL

Materials

All chemical used in this research, including phosphoric acid (H_3PO_4, 99%), hydrochloric acid (HCl, 99%), safranin, titanium dioxide nanoparticles (TiO_2NP_S), rutile and chitosan were ordered from Merck (Darmstadt, Germany) with high purity.

Methods

Synthesis of activated carbon. The activated carbon has been prepared based on the reported method in the previous work [11]. Persian mesquite grains were chosen for activated carbon due to their low ash content and high amount of volatile materials which gives a suitable feedstock for activated carbon. Dried raw Persian mesquite grains powders were mixed with H_3PO_4 solution (1:1) and were dried at 105 °C for 12 h. The pyrolysis of obtained material was done in a stainless steel reactor from room temperature to 600 °C with a heating rate of 7 (°C min^{-1}) under N_2 flow and continued at 600 °C for 100 min. The result activated carbon was cooling down and was boiled in 200 ml of 10% HCl solution for 60 min, then was filtered

and washed with distilled water to eliminate inorganic species. Finally, activated carbon was then dried in an oven overnight at 100 °C.

Synthesis of AC loaded with TiO_2NP_S. AC/TiO_2NP_S was obtained by magnetic stirring titanium with activated carbon in a ratio of 1:10 at 25 °C for ten h until loading of TiO_2NP_S on the AC was completed. Then the solution was centrifuged. The centrifuged Ac/TiO_2 particles were dispersed by ultrasonic for one hour and dried in an oven at 80 °C [12].

Synthesis of Ac/TiO_2 loaded with chitosan. Chitosan was mixed with Ac/TiO_2NP_S solution with a 2:10 ratio for ten h at 25 °C under magnetic stirring until the chitosan covered the Ac/TiO_2 surface and centrifuged. Then the centrifuged Ac/TiO_2/Ch particles were dispersed by ultrasonic for one h and were dried at 80 °C in an oven [12].

Instruments

The instruments that were used in this work, for studying the structural properties and absorption processes, are UV-Vis spectrophotometer model V-570, Scanning electron microscope (FESEM, MIRA3 LMU MI2851376IR model), Perkin Elmer TGA Piers' 1 analyzer. Also, for BET measurement of surface area, pore size, and volume distribution, Specific Surface Area and Porosity Analyzer (PHS-1020(PHSCHINA) was used.

Batch Adsorption

Initially, in a volumetric flask, the stock solution with 1000 ppm safranin o was prepared by dissolving the needed amount of safranin o, and then more diluted solutions were made to get specific dye concentrations. A shaker incubator was used for adsorption experiments at identified temperature and 175 rpm. Removal percent of the safranin o were studied at different times, pH, adsorbent amount, temperature, and initial dye concentration. Equation (1) has been used to calculate the removal percentage of safranin o:

$$\%R_e = \frac{C_0 - C_e}{C_0} \times 100 \quad (1)$$

where R_e, C_0 and C_e are the removal percentage, initial, and equilibrium concentrations of safranin o, respectively. In the above equation, C_0 and Ce are in mg l^{-1}. q_e (the amount of maximum equilibrium adsorption capacity (mg g^{-1})) was determined by the Eq. (2):

$$q_e = \frac{(C_0 - C_e)V}{W} \quad (2)$$

In above equation, the C_e (mg l^{-1}), V (l) and W (g) parameters are the dye's concentration at equilibrium, the volume of the solution, and the adsorbent weight, respectively.

RESULTS

Characterization of Adsorbents

The thermogravimetric technique (TGA) is generally applied to determine the change in the component during surface modification. Figure 2 shows the TGA thermogram details of Ac/$TiO_2$and Ac/TiO_2/Ch composites. The figure shows two and three stages of decomposition for Ac/TiO_2 and Ac/TiO_2/Ch. The first thermal peak, between 84.9 ºC with a weight loss of 8.93 wt.%, is probably due to the endothermic removal of physically and chemically adsorbed water from the composite (Fig. 2a) [13]. The second weight loss in Fig. 2a at a temperature between 378-780 ºC (77.63% weight) indicate the loss of hydroxyl groups on the TiO_2 nanocrystal and decomposition of amorphous carbon layers. The mass, which approximately keeps constant after 600 ºC, contains the loaded TiO_2NP_S and ash in AC [13,14]. The first weight loss in Fig. 2b in the 87.1 ºC (28.30 wt.%) shows the loss of water or the vaporization of remain solvents in prepared samples [15,16]. The second stage in Fig. 2b, between 149.9 ºC-380 ºC (19.18% weight), represents the scission of the polymer chains. The third peak, occurs at a temperature between 543.6-920 ºC, is due to breakdown of the polymeric molecule chains. These results show that thermal stability of Ac/TiO_2/Ch composite is considerably more than that of Ac/TiO_2composite [17]. Therefore, from the TGA results, it can be understood that TiO_2NP_S and chitosan were successfully placed onto activated carbon.

FT-IR spectra of the samples are reported in Fig. 3 to study variation in the functional groups. As can be observed, the peaks of the Ac spectrum are weaker than that of the raw material (RM) spectrum and/or have been

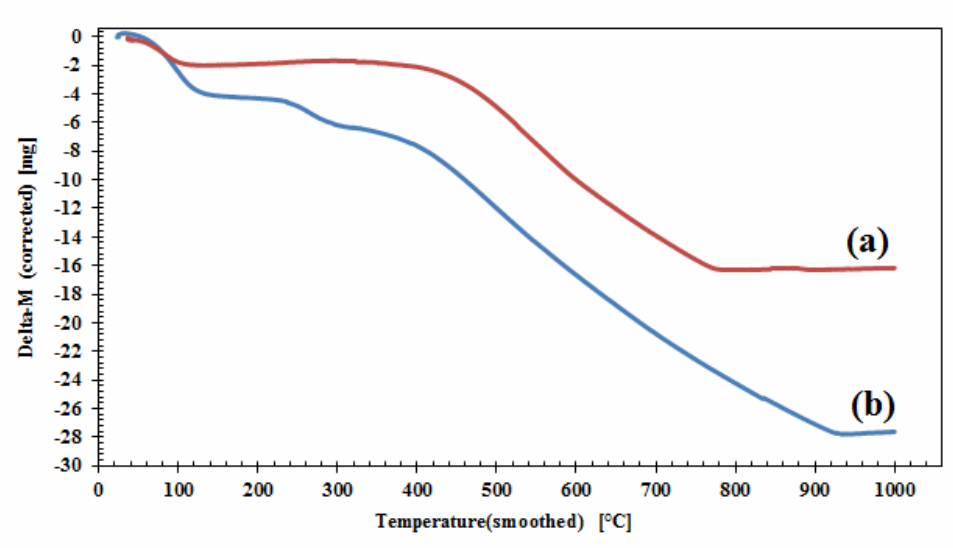

Fig. 2. TGA curves of (a) Ac/TiO_2 and (b) Ac/TiO_2/Ch nanocomposites.

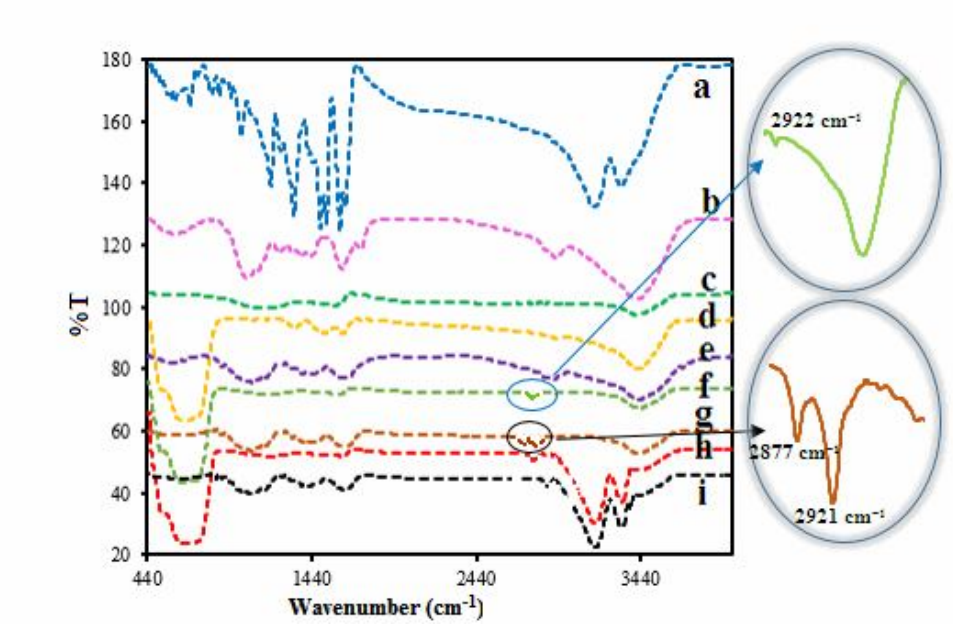

Fig. 3. The FT-IR results of a) safranin o, b) RM, c) AC, d) TiO_2NPS, e) Ch, f) Ac/TiO_2, g) Ac/TiO_2/Ch, h) Ac/TiO_2 after safranin o adsorption and i) Ac/TiO_2/Ch after safranin o adsorption.

removed after the activation process (450-600 and 9500-1700 cm^{-1}). This confirms that the elimination of some functional groups in the RM could be due to the carbonation and activation steps [18]. Comparing the FT-IR spectra of TiO_2NPS with TiO_2NPS/AC and Ch/TiO_2NPS/AC adsorbents, indicates the presence of bands at about 400-800 cm^{-1} in the final samples (Ac/TiO_2 and Ac/TiO_2/Ch adsorbents); these peaks were attributed to the Ti–O-Ti and, or Ti–O bonds [19]. Also, a transition band represents the composite band (2922 cm^{-1}) TiO_2NPS in Ac/TiO_2/Ch

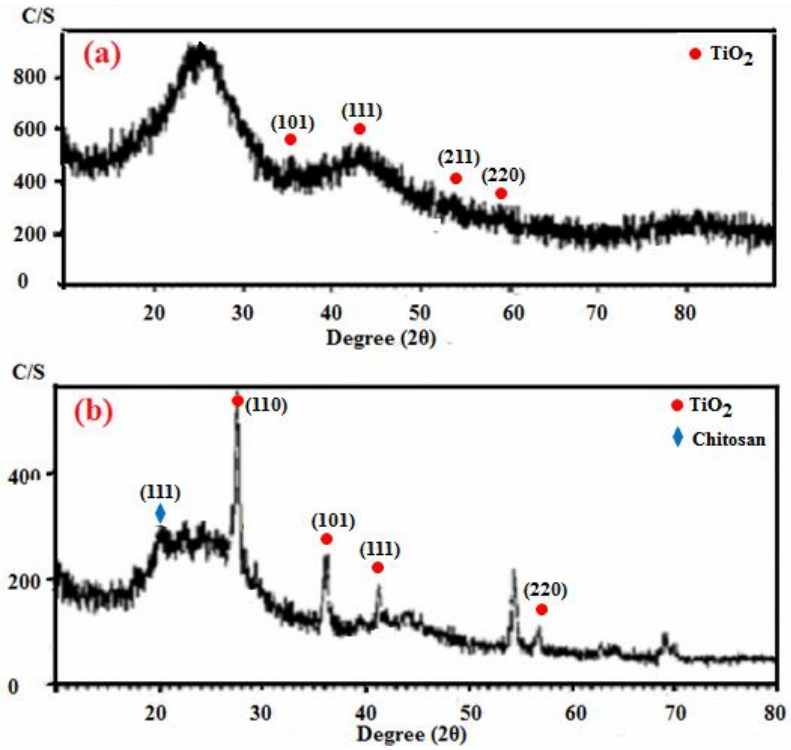

Fig. 4. XRD pattern of the (a) Ac/TiO_2 and (b) Ac/TiO_2/Ch nanocomposites.

and Ac/TiO_2 adsorbents, confirming that TiO_2NPS were loaded in AC [20,21]. In the spectra related to Ac/TiO_2/Ch, the N–H and O–H stretching bands have appeared in the 3291-3361 cm^{-1}. Bands in the regions 2877 and 2921 cm^{-1} are associated with C–H asymmetric and symmetric stretching, respectively. Also these bonds have similar spectra with polysaccharides, for example, carrageenans [22], glucans [23] and xylan [24], therefore they have characteristics of polysaccharide. The presence of primary amine was confirmed by the N–H bending peak at 1589 cm^{-1}. Also, bands at around 1423 and 1375 cm^{-1} correspond to the CH_2 bending and CH_3 symmetrical deformations, respectively. The bands at 1066 and 1028 cm^{-1} can be attributed to C–O stretching. The band at 1153 cm^{-1} corresponds to the asymmetric stretching of the C–O–C bridge. The bands that appeared in the chitosan Ac/TiO_2/Ch spectrum were found to be consistent with the previously reported results [25,26]. The two prominent peaks of the safranin o at 3183 and 3338 cm^{-1} correspond to $–NH_2$ and –OH groups, respectively. The presence of these peaks on the Ac/TiO_2 and Ac/TiO_2/Ch in the FT-IR spectra of samples after safranin o adsorption indicates that the adsorption process has been successful [27].

Figures 4a and 4b display the XRD pattern of TiO_2NP_S, and TiO_2/Ch coated onto activated carbon prepared by Persian mesquite grain. In these patterns, activated carbon could not be recognized because of its amorphous structure. However, it is well understood that the TiO_2NP_S have a crystalline structure [28]. As Fig. 4a shows, the peak at around $2\theta = 27°$ can be due to the interaction of TiO_2NP_S with surface functional groups, and the reduction in crystallinity of Ac can be attributed to the loading of TiO_2NP_S [29]. In this sample, planes 101, 111, 211 and 220 are related with the peaks at 2θ = 36.12, 41.31, 54.33 and 56.63°, respectively. This result is in good agreement with the previous works reported in literature [30,31]. The appearance of similar peaks and also plane 110 at $2\theta = 27°$ in sample Ac/TiO_2/Ch indicates that the TiO_2NPS are well prepared within the AC (Fig. 4b). The XRD pattern of Ac/TiO_2/Ch is shown in Fig. 4b. There is a broad peak at

Table 2. Porous Structure Parameters

Adsorbent	S_{BET} ($m^2\ g^{-1}$)	V_m ($cm^3\ g^{-1}$)	Average pore diameter (nm)
Ac/TiO_2	773.15	201.143	3.242
$Ac/TiO_2/Ch$	834.477	214.512	2.303

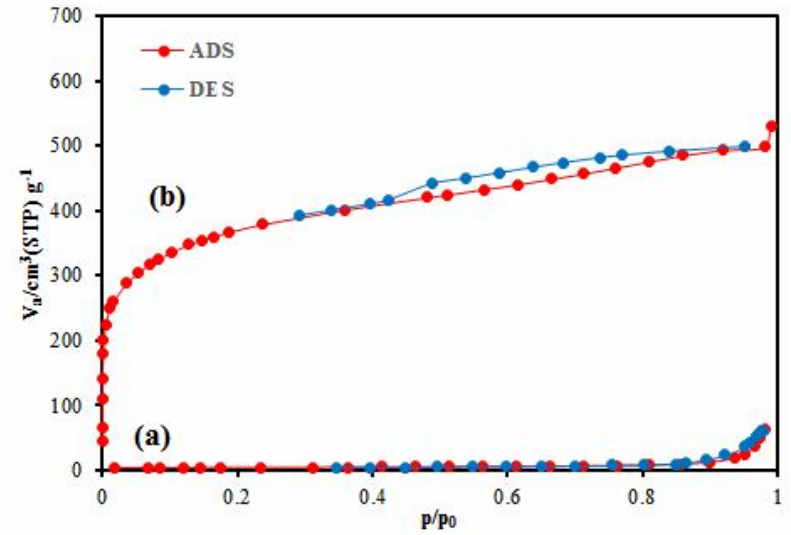

Fig. 5. Adsorption/desorption isotherm of (a) Ac/TiO_2 and (b) $Ac/TiO_2/Ch$) nanocomposites.

$2\theta = 20^\circ$ related to plane 111, which is evidence of partial crystallinity of the chitosan specimen [32]. Also, the peaks at about $2\theta = 44°$ confirmed the presence of TiO_2-rutile onto activated carbon [33]. Furthermore, in Fig. 4b, the peaks associated with TiO_2NP_S appeared at $2\theta = 27°$, 36° and 44°; the higher intensity of TiO_2NP_S peak demonstrate an increase in the availability of TiO_2NP_S [34].

Some essential parameters related to the porosity of prepared adsorbents, including micropore volume, total pore volume, and average pore radius of Ac/TiO_2 and $Ac/TiO_2/Ch$, are mentioned in Table 2. Based on results in Table 2, the Ac/TiO_2 and $Ac/TiO_2/Ch$ show BET surface area of 773.15 ($m^2\ g^{-1}$) and 834.477 ($m^2\ g^{-1}$), respectively. The $Ac/TiO_2/Ch$ shows a higher surface area, micropore, and total pore volume than Ac/TiO_2. According to the standard definition of IUPAC, the pore size < 2 nm, 2-50 nm, and >50 are related to the micropore, mesopore, and macropore, respectively [35], both different adsorbent Ac/TiO_2 and $Ac/TiO_2/Ch$ have mesoporous (2-50 nm) structures. Figure 5a and Fig. 5b present the N_2 adsorption-desorption of Ac/TiO_2 and $Ac/TiO_2/Ch$, respectively.

A scanning electron microscope (SEM) image gives information related to the surface and particle size distribution. SEM images of the raw material, activated carbon, Ac/TiO_2, and $Ac/TiO_2/Ch$ are given in Figs. 6. Figure 6a displays the almost smooth and homogeneous surface of the AC. It can be seen from Fig. 6b that the surface of AC were damaged and many cavities were appeared; this shows the expansion of pores structure after the activation procedure. An SEM image of TiO_2NP_S coated onto activated carbon is shown in Fig. 6c. This figure illustrates that the sizes of the TiO_2NP_S are ranged from 20-39 nm, and are uniformly developed on the entire AC surface. Also, SEM images display an uneven morphology

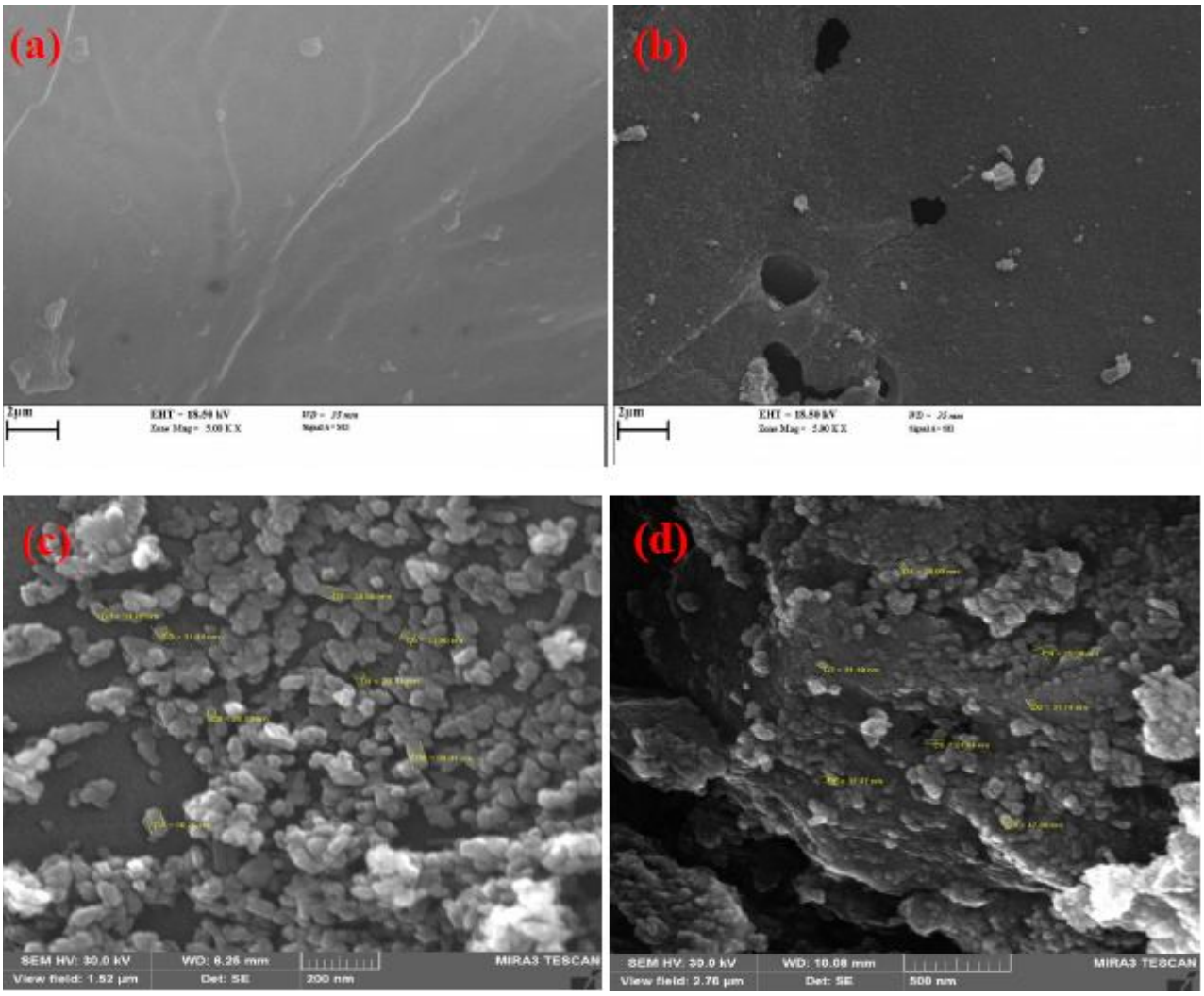

Fig. 6. SEM images of (a) raw material and (b) activated carbon (c) Ac/TiO_2 (d) Ac/TiO_2/Ch.

with a large number of macropores and an irregular surface that confirm loading of TiO_2NP_S/Ch onto activated carbon and the formation of Ac/TiO_2/Ch nanocomposite (Fig. 6d). This figure shows that the sizes of the Ac/TiO_2/Ch nanocomposite are ranged from 29.83-50 nm.

Safranin o Removal by Ac/TiO_2 and Ac/TiO_2/Ch Adsorbents

Effect of pH. The solution's pH is a necessary factor for the adsorption of dye that affects the interaction of adsorbent with adsorbate by changing the surface charge of the components [36]. Figure 7 shows the effect of pH of solution on the safranin o adsorption by Ac/TiO_2 and Ac/TiO_2/Ch adsorbents investigated at 298 K and different pH ranges of 2-10. The results show that the removal percentage of the safranin o solution efficiency increased by an increase in pH. At a lower pH (acidic pH), the surface of Ac/TiO_2 and Ac/TiO_2/Ch show more positive charge and less removal percentage. The reduction in the removal percentage in acidic pH could be related to the competition process between dye cations and H^+ ions of the surfaces of Ac/TiO_2 and Ac/TiO_2/Ch adsorbents. However, in a higher

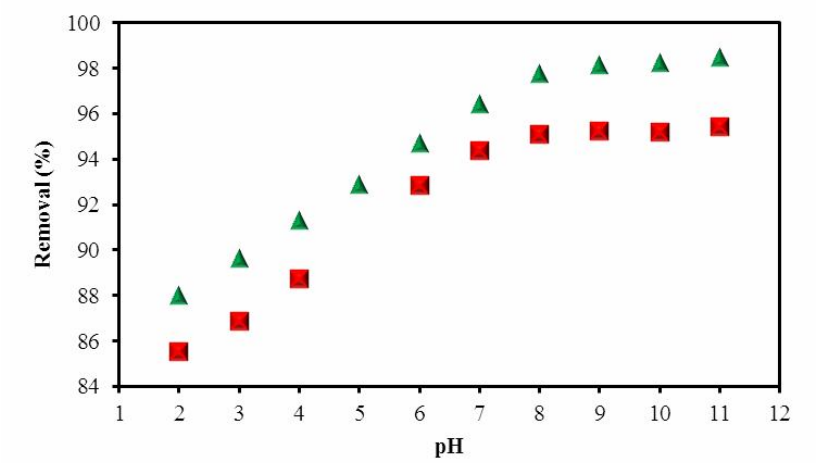

Fig. 7. Effect of solution's pH on the removal of safranin o by (▲) Ac/TiO_2; (■) Ac/TiO_2/Ch adsorbents.

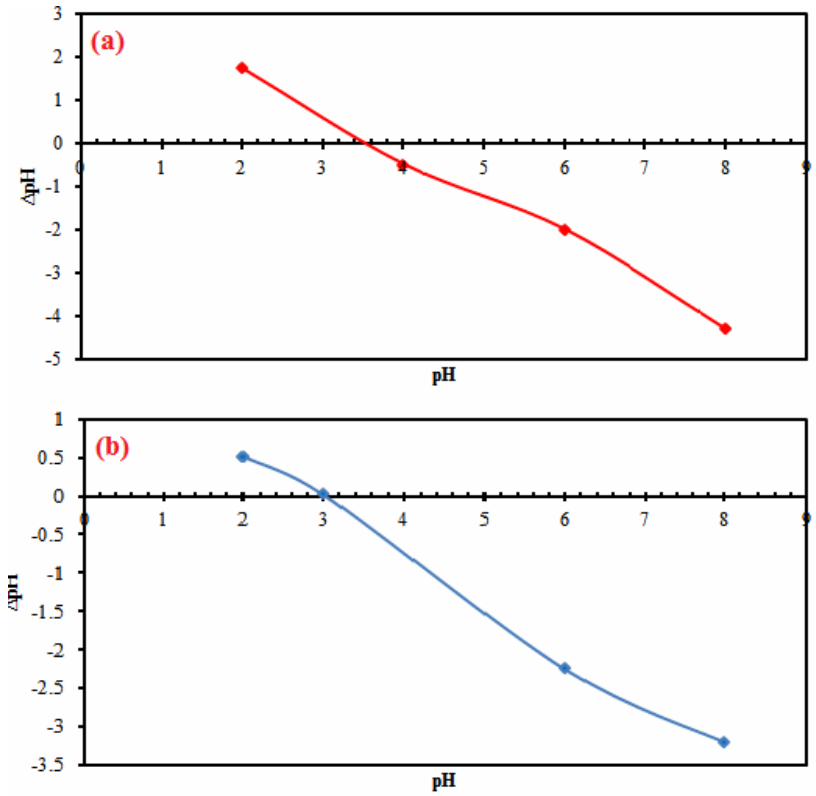

Fig. 8. pH_{PZC} of (a) Ac/TiO_2, and (b) Ac/TiO_2/Ch adsorbents.

amount of pH, the percentage removal of safranin o is high due to the opposite charge of the dye molecules and the adsorbent's surface [37,38].

Based on the point of zero charges (PZC), in the present study, the pH values for the zero charged Ac/TiO_2 and Ac/TiO_2/Ch were found to be approximately pH = 3.54 and 3, respectively, As shown in Fig. 8, the pH_{PZC} was calculated based on the ΔpH (pH_{final} - $pH_{initial}$) = 0 for the

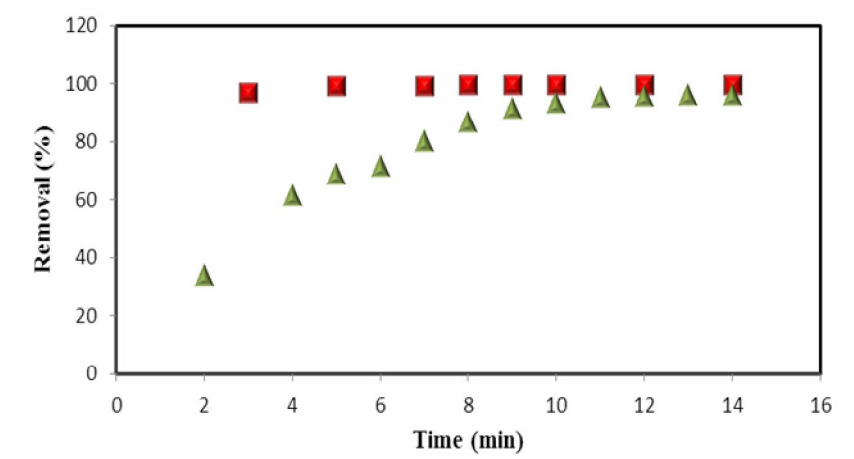

Fig. 9. The effect of contact time on the removal of safranin o by (▲) Ac/TiO_2; (■) Ac/TiO_2/Ch adsorbents.

both adsorbents. Therefore, at pH higher than pH_{pzc}, the adsorbent surface is negatively charged and adsorbs the safranin o dye *via* electrostatic attraction. In other words, at the lower amount of pH (acidic pH), the surface of Ac/TiO_2 and Ac/TiO_2/Ch) is more positively charged and less removal percentage is obtained. The reduction in removal percentage in acidic pH is related to the competition process between dye Cations and H^+ ions of surfaces of Ac/TiO_2 and Ac/TiO_2/Ch adsorbents. However, in higher ranges of pH, the percentage removal of safranin o is high due to the opposite charge of the dye molecules and the surface of the adsorbent [39]. Similar behavior was observed for the adsorption of methylene violet and methyl orange onto Phragmites australis [40] and methylene blue onto AC [18].

The contact time effect. The mixing time is one of the effective parameters in the adsorption process [41]. To observe the effect of contact time on the safranin o adsorption capacity, a simple comparison was made between Ac/TiO_2 and Ac/TiO_2/Ch adsorbents. Figure 9 shows the removal of safranin o from the Ac/TiO_2 and Ac/TiO_2/Ch adsorbents at different times. Base on the plots, the best removal of dye is occurred after 25 and 35 min for the Ac/TiO_2/Ch and Ac/TiO_2, respectively. The high rate of removal in the adsorption process was associated with available vacant surface sites for adsorption. At the equilibrium time, adsorption is nearly constant due to the saturation of adsorbent sites [35,44]. Comparing the results of safranin o removal at different times confirmes the highly effective performance of the adsorbents for the removal of safranin o dye.

The adsorbent amount effect. The amount of adsorbent has been studied as an influential factor on adsorbent and adsorption ability. The removal percentage of safranin o as a function of the adsorbent amount was studied at constant time, pH, initial concentration, and temperature. The results are demonstrated in Fig. 10. The results confirm the increase of safranin o removal percentage with an increase in adsorbents dose until remained nearly constant. This behavior arises from the availability of more adsorption sites due to an increase in the adsorbents surface area. The latter change is due to an increase in amount of the adsorbents, and the adsorbent amount increased when the adsorption density of safranin o dye decreased [33].

The initial safranin o concentration effect. To investigate the role of initial concentration on adsorption studies, the initial concentration ranges of 20-80 mg l^{-1} are studied in this work. As Fig. 11 shows, the removal percentage increased with an increase in dye concentration. This behavior is related to the accessibility of unoccupied surface active sites [6]. The adsorption at high concentration increased due to the increased repulsion between the adsorbent and the adsorbed molecules, and also due to slow saturation of the pores. Furthermore, according to Fig. 11, the Ac/TiO_2/Ch nanocomposite has higher absorption capacity than Ac/TiO_2. The Ac/TiO_2/Ch nanocomposite is an excellent adsorbent for removal of most pollutants due to

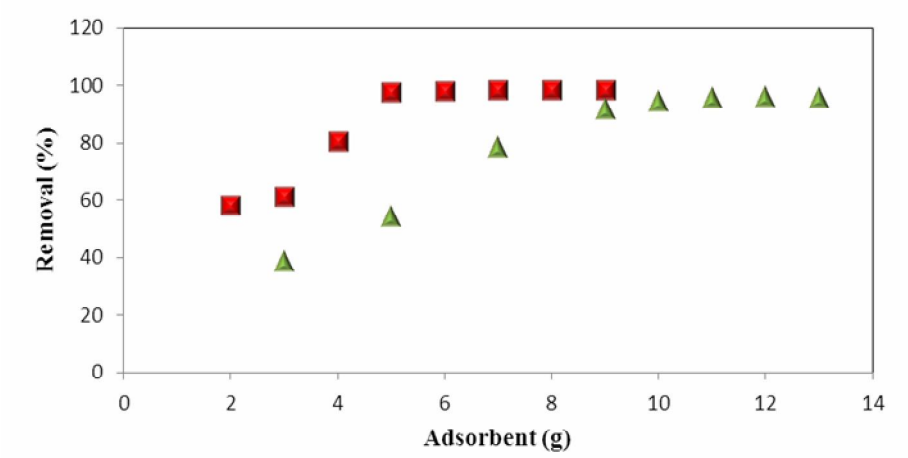

Fig. 10. The Effect of adsorbent dose on the removal of safranin o by (▲) Ac/TiO_2; (■) Ac/TiO_2/Ch adsorbents.

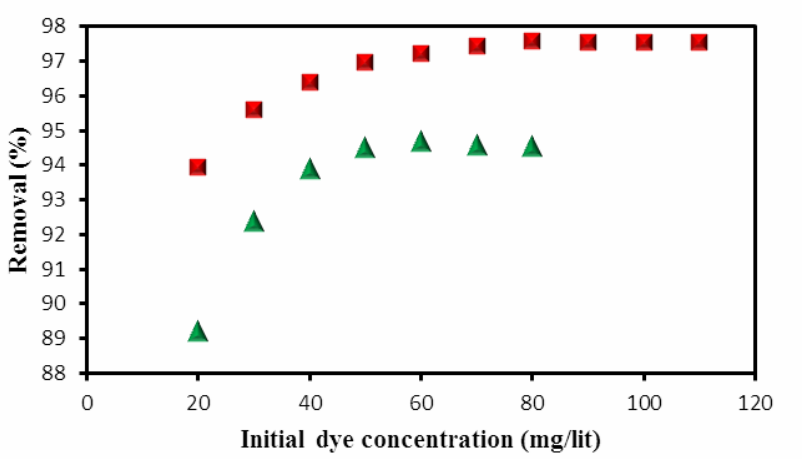

Fig. 11. The effect of initial concentration on the removal of safranin o by (▲) Ac/TiO_2; (■) Ac/TiO_2/Ch adsorbents.

its excellent surface area. In general, these results indicate that the loading of TiO_2NP_S/Ch onto the surface of Ac has led to an increase in its special surface area and reactive sites.

The temperature effect. To study the exothermic or endothermic nature of the adsorption process, the safranin o dye removal, the effect of temperature was investigated by performing the process at different temperatures between 293.15-288.5 K. The presented results in Fig. 12 shows that the adsorption of safranin o by the Ac/TiO_2 and Ac/TiO_2/Ch is expanded as the temperature increases, which indicates the adsorption process is endothermic. Also, the strong interaction between safranin o molecule and the adsorbent molecules is due to the increase in temperatures with increased adsorption.

Adsorption Isotherm

In this research, experimental data for dye removal from the two adsorbents were analyzed using famous adsorption isotherms, for example, Langmuir [43], Freundlich [44], Temkin [45] and Dubinin Radushkevitch (D-R) [46]. The Langmuir adsorption isotherm, developed by Irving Langmuir in 1916; he suggested that the adsorption process is monolayer and the adsorption sites are homogenous. The

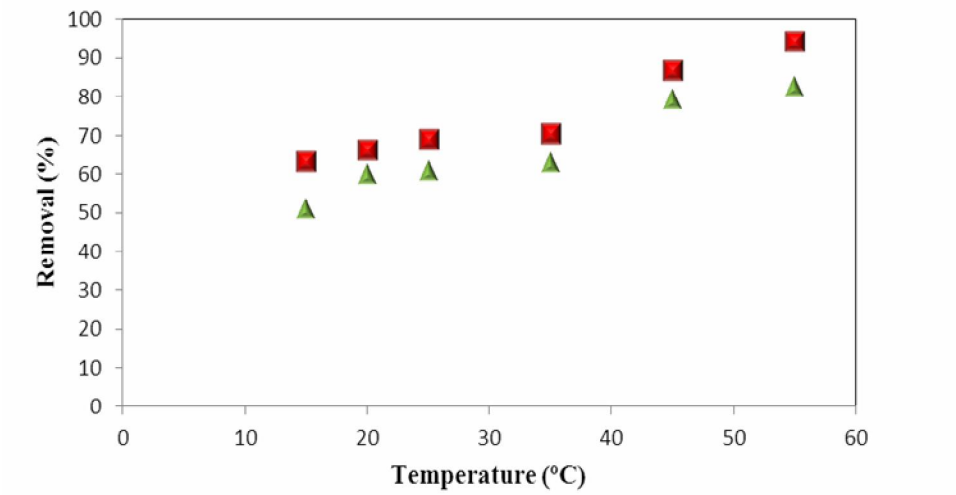

Fig. 12. The effect of temperature on the removal of safranin o by (▲) Ac/TiO_2; (■) $Ac/TiO_2/Ch$ adsorbents.

Table 3. Isotherm Constant and Correlation Coefficients Calculated for Safranin o Adsorption

Isotherm	Parameters	Ac/TiO_2	$Ac/TiO_2/Ch$
Langmuir	Q_m (mg g^{-1})	166.66	357.14
	K_l (l mg^{-1})	0.115	0.166
	R^2	0.88	0.95
Freundlich	1/n	1.151	1.028
	K_f (l mg^{-1})	27.915	34.389
	R^2	0.92	0.90
Tempkin	B_1	0.0063	0.0044
	K_T (l mg^{-1})	4.30E + 32	1.48E + 63
	R^2	0.96	0.99

linear form of this model is presented as follow:

$$\frac{C_e}{q_e} = \frac{1}{L_L q_m} + \frac{C_e}{q_m} \quad (3)$$

In above equation, q_m and K_L are the maximum adsorption capacity (mg g^{-1}) and the Langmuir adsorption constant (l mg^{-1}), respectively. q_m (slope) and K_L (intercept) constants were calculated from the plot of $1/q_e$ *vs*. C_e.

Table 3 shows the calculated results, including correlation coefficients and constants in this model. According to this Table, for the Langmuir model, the correlation coefficients (R^2) are 0.99 and 0.97 and the maximum adsorption capacities (q_m) are 139 and 164 mg g^{-1} for Ac/TiO_2 and $Ac/TiO_2/Ch$ adsorbents, respectively. These values indicate that Ac/TiO_2 and $Ac/TiO_2/Ch$ are good candidates for removal of safranin o.

The following shows the used isotherm in this work that is a

model introduced by Freundlich. This isotherm assumes that the surface is heterogeneous. The common form of this isotherm presented in Eq. (4):

$$\log q_e = \log K_f + \frac{1}{n}\log C_e \quad (4)$$

n and K_f are the Freundlich constants that reveal the adsorption intensity and relative capacity, respectively. The adsorption procedure is chemical if $n < 1$, and is physical if $n > 1$. The correlation coefficient R^2 (the plot of $\log q_e$ *vs.* $\log C_e$) was obtained to be 0.93 and 0.89 for Ac/TiO_2 and Ac/TiO_2/Ch adsorbents, respectively (see Table 3). According to the presented results in Table 3, the 1/n values were 0.35 and 0.38 for Ac/TiO_2 and Ac/TiO_2/Ch adsorbents, respectively. From the Freundlich perspective, the results indicate that Ac/TiO_2 and Ac/TiO_2/Ch adsorbents have a high degree of heterogeneity.

The adsorption data for adsorption over Ac/TiO_2 and Ac/TiO_2/Ch were also discussed by linear Temkin, and Pyzhev equation. The linear equation is the following:

$$q_e = B_1 \ln K_T + B_1 \ln C_e \quad (5)$$

This equation displays the effects of adsorbate/adsorbate interactions on adsorption isotherms. In Eq. (5), B_1 (= RT/b) is the heat of adsorption, K_T is the binding energy of the adsorbent and adsorbate, R (8.314 J K^{-1} mol^{-1}) is the universal gas constant, and T (K) is the absolute temperature. The values of B_1 and K_T were calculated from the plot of q_e against lnCe, respectively (Table 3). According to the reported data in Table 3, it can be concluded that the Ac/TiO_2 adsorbent is better fitted with the Langmuir isotherm model and the Ac/TiO_2/Ch adsorbent is more fitted with the Freundlich isotherm model; this means that these two models are the most likely isotherm that can explain the adsorption process in aqueous solution.

Kinetics of Adsorption

The kinetics of adsorption gives us information about the applicability of adsorbents and the mechanism of adsorption. In this study, kinetics models including the pseudo-first-order (Lagergren and Svenska) [47], pseudo-second-order (Ho and Mckay) [48], and Elovich (Elovich and Larionov) [49] have been used to evaluate the kinetic data to figure out the kinetic mechanism.

Equation (6) shows the first-order kinetic model (linear form) [47]:

$$\log(q_e - q_t) = \log q_e - \frac{K_1 t}{2.303} \quad (6)$$

In this equation, adsorption capacities at time (t) and at equilibrium are shown with q_t (mg g^{-1}) and q_e (mg g^{-1}), respectively; and k_1 is the pseudo-first-order rate constant (min^{-1}) that can be determined using the plot of $\log(q_e - q_t)$ *vs.* t (Table 4).

The pseudo-second-order equation is shown by the following equation [8]:

$$\frac{t}{q_t} = \frac{1}{K_2 q_e^2} + \frac{1}{q_e(t)} \quad (7)$$

Using the plot of t/q_t *vs.* t, the values of K_2, q_e and R^2 were calculated and the results have been summarized in Table 4. According to these parameters, we conclude that this model is in good agreement with the experimental data. This fact shows that the sorption of safranin o on Ac/TiO_2 and Ac/TiO_2/Ch is based on the pseudo-second-order model.

The next kinetic model is the Elovich kinetic model with equation:

$$q_t = \frac{1}{\beta}\ln \alpha\beta + \frac{1}{\beta}\ln t \quad (8)$$

Where q_t [mg (g min)$^{-1}$], α and β are the amounts of adsorbed dye by an adsorbent at time t, the initial dye adsorption rate, and the desorption constant (g mg^{-1}) during each experiment, respectively. According to the parameters mentioned in Table 4, the Elovich model failed to describe the kinetics of the adsorption process.

The data clearly show that the pseudo-second-order kinetic is in excellent agreement with experimental data, because the best linearity is obtained; the value of R^2 are 0.99 and 1 for Ac/TiO_2, and Ac/TiO_2/Ch, respectively, which are higher than the corresponding values calculated for the other models. Since the pseudo-second-order model is the driving force, the rate of adsorption, which explains

Table 4. Adsorption Kinetic Parameters for Safranin o Adsorption onto Ac/TiO_2 and $Ac/TiO_2/Ch$

Model	Parameter	Ac/TiO_2	$Ac/TiO_2/Ch$
First-order	q_e	3.98	1.60
	$K_1 \times 10^{-3}$ ($l\ min^{-1}$)	0.122	0.156
	R^2	0.99	0.83
Second-order	q_e	28.55	384.89
	$K_2 \times 10^{-3}$ ($l\ min^{-1}$)	0.079	0.0009
	R^2	0.99	1
Elovich	b	12.57	0.520
	a	0.962	251.84
	R^2	0.97	0.69
Intraparticle	K_{dif} ($l\ min^{-1}$)	0.478	0.654
	C	1.01	1.10
	R^2	0.88	0.99

Table 5. Thermodynamic Parameters for Safranin o Adsorption onto Ac/TiO_2 and $Ac/TiO_2/Ch$

Adsorbate	Parameter	Temperature (K)					
		288.15	293.15	298.15	308.15	318.15	328.15
Ac/TiO_2	Kº	3.4525	3.9418	4.4913	4.8100	13.3517	33.8523
	ΔGº (kJ mol^{-1})	-2530.38	-2897.22	-3269.99	-2555.25	-6369.91	-9107.3
	ΔHº (kJ mol^{-1})	-5664					
	ΔSº (kJ mol^{-1})	20.727					
$Ac/TiO_2/Ch$	Kº	3.4897	5.0220	5.2548	5.7171	12.8804	15.8327
	ΔGº (kJ mol^{-1})	-7091.78	-6554.62	-6154.43	-5582.11	-5182.05	-4881.12
	ΔHº (kJ mol^{-1})	-3544.5					
	ΔSº (kJ mol^{-1})	13.616					

that the mechanism of adsorption of safranin by Ac/TiO_2, and $Ac/TiO_2/Ch$ is a pseudo-second-order kinetic mechanism, it is confirmed that the rate-limiting step is chemisorption. Meanwhile, the pseudo-second-order model describes the external liquid diffusion, surface adsorption, and intra-particle diffusion processes. This model provided a more comprehensive and accurate reflection of the adsorption mechanism of safranin onto the adsorbent than the pseudo-first-order model.

Adsorption Thermodynamics

In order to calculate the Gibbs free energy change of the adsorption process, the Eq. (9) was used:

$$\Delta G^{\circ} = -RT \ln K_c \tag{9}$$

where R (8.314 J mol^{-1} K^{-1}), T (K), and K_c display the universal gas constant, temperature, and equilibrium constant, respectively. The K_c constant in Table 5 has been

Table 6. Comparison of The maximum Adsorption Capacity (Q_m) of Ac/TiO_2/Ch Adsorbent with Adsorbents Found in the Literature for Safranin o Adsorption

Sorbent	Q_m (mg g^{-1})	Ref.
Ac/TiO_2/Ch	357.14	This paper
Magnetic fluid modified peanut husks	86.1	[50]
Chlorella vulgaris	115	[51]
Magnetically modified Sargassum horneri biomass	144.4	[52]
MgO decked multi-layered graphene	3.929×10^{-4}	[6]
Sugar beet pulp	147	[53]
Calcined bones	107.8	[54]
Aagro-waste material soybean hull	14.99	[38]
Spent coffee grounds	59	[55]

obtained using the graph of the q_e/C_e *vs*. q_e. The calculated value of ΔGº was negative, and hence, it shows that the adsorptions of safranin o by Ac/TiO_2, and Ac/TiO_2/Ch adsorbents are spontaneous in nature. In the Van't Hoff equation (Eq. (10)), the slope and intercept of lnK° *vs*. 1/T calculated to obtain the standard entropy changes (ΔSº) and enthalpy changes (ΔH°) for adsorption, respectively.

$$\ln K^{\circ} = \frac{\Delta S^{\circ}}{R} - \frac{\Delta H^{\circ}}{RT} \quad (10)$$

The ΔHº values of Ac/TiO_2 and Ac/TiO_2/Ch adsorbents are negative, so the adsorption is exothermic. Also, the positive values of ΔS° show an increase in the disorder (or degree of freedom) of the adsorbed molecules.

COMPARISON OF AC/TIO$_2$/CH ADSORBENT WITH SOME DATA OBTAINED FROM OTHER SORBENTS

The described adsorbent in this paper for dye removal is an inexpensive material that has been synthesized and modified with a straightforward method. Comparison of the maximum adsorption capacity (Q_m) of Ac/TiO_2/Ch adsorbent for safranin o adsorption with that of other adsorbents found in the literature (see Table 6) indicatesthe excellent Q_m of the Ac/TiO_2/Ch.

CONCLUSIONS

The adsorption of safranin o cationic dye from the water on Ac/$TiO_2$and Ac/TiO_2/Ch adsorbents was investigated. The Ac/TiO_2/Ch adsorbent showed an excellent adsorption capacity for removal of safranin o cationic dye. The Langmuir isotherm model successfully described the equilibrium adsorption data. Also, the kinetic data for the Ac/TiO_2 and Ac/TiO_2/Ch adsorbents were fitted using the pseudo-second-order model. This work indicates that Ac/TiO_2 can be considered as a novel and excellent adsorbent due to its high adsorption capacity and low equilibrium time. The pseudo-second-order kinetic model successfully explained the safranin o removal process by the adsorbent, hence, the mechanism of adsorption of safranin by Ac/TiO_2 and Ac/TiO_2/Ch has pseudo-second-order kinetic mechanism, and therefore, the rate-limiting step is chemisorption.

The calculated thermodynamic adsorption parameters showed that the adsorptions of safranin o dye onto Ac/TiO_2 and Ac/TiO_2/Ch adsorbents are spontaneous and exothermic under the experimental conditions.

ACKNOWLEDGMENTS

The authors are grateful for the facilities and the financial assistance received from the Research Councils of

the Shahid Chamran University of Ahvaz.

CONFLICTS OF INTEREST

The authors declare that they have no known competing financial interests or personal relationships that could have appeared to influence the work reported in this research paper.

REFERENCES

[1] Tanhaei, B. A.; Sillanpää, M., Magnetic xanthate modified chitosan as an emerging adsorbent for cationic azo dyes removal: Kinetic, thermodynamic and isothermal studies. *Int. J. Biol. Macromol.* **2019**, *12*, 1126-1134, DOI: 10.1016/ j.ijbiomac.2018.10.137.

[2] Malik, P.; Saha, S., Oxidation of direct dyes with hydrogen peroxide using ferrous ion as catalyst. *Sep. Purif Technol.* **2003**, *31*, 241-250, DOI: 10.1016/ S1383-5866(02)00200-9.

[3] Walker, G., Kinetics of a reactive dye adsorption onto dolomitic sorbents. *Watr Res.* **2003**, *37*, 2081-2089, DOI: 10.1016/S0043-1354(02)00540-7.

[4] Chen, K. C., Decolorization of the textile dyes by newly isolated bacterial strains. *J. Biotechnol.* **2003**, *101*, 57-68, DOI: 10.1016/S0168-1656(02)00303-6.

[5] Lin, S. H.; Peng, C. F., Continuous treatment of textile wastewater by combined coagulation, electrochemical oxidation and activated sludge. *Water Res.* **1996**, *30*, 587-592, DOI: 10.1016/0043-1354(95)00210-3.

[6] Rotte, N. K., Equilibrium and kinetics of Safranin O dye adsorption on MgO decked multi-layered graphene. *Chem. Eng. J.* **2014**, *258*. 412-419, DOI: 10.1016/j.cej.2014.07.065.

[7] Vukčević, M. M., Production of activated carbon derived from waste hemp (Cannabis sativa) fibers and its performance in pesticide adsorption. *Microporous Mesoporous Mater.* **2015**, *214*, 156-165, DOI: 10.1016/j.micromeso.2015.05.012.

[8] Hydari, S., A comparative investigation on removal performances of commercial activated carbon, chitosan biosorbent and chitosan/activated carbon composite for cadmium. *Chem. Eng. J.* **2012**, *193*, 276-282, DOI: 10.1016/j.cej.2012.04.057.

[9] Thamaphat, K.; Limsuwan, P.; Ngotawornchai, B., Phase characterization of TiO_2 powder by XRD and TEM. *Agric. Nat. Resour.* **2008**, *42*, 357-361.

[10] Ngah, W. W.; Teong, L.; Hanafiah, M. M., Adsorption of dyes and heavy metal ions by chitosan composites: A review. *Carbohydr. Polym.* **2011**, *83*, 1446-1456, DOI: 10.1016/j.carbpol.2010.11.004.

[11] Ghasemian Lemraski, E.; Sharafinia, S.; Alimohammadi, M., New activated carbon from Persian mesquite grain as an excellent adsorbent. *Phys. Chem. Res.* **2017**, *5*, 81-98, DOI: 10.22036/pcr.2017.38495.

[12] Ao, Y., Low temperature preparation of anatase TiO2-coated activated carbon. *Colloids Surf. A Physicochem. Eng. Asp.* **2008**, *312*, 125-130, DOI: 10.1016/j.colsurfa.2007.06.039.

[13] Rosa, S., Non-synergistic UV-A photocatalytic degradation of estrogens by nano-TiO_2 supported on activated carbon. *J. Brazil Chem. Soc.* **2017**, *28*, 582-588, DOI: 10.5935/0103-5053.20160201.

[14] Xing, B., Preparation of TiO_2/activated carbon composites for photocatalytic degradation of RhB under UV light irradiation. *J. Nanomater.* **2016**, 11-20, DOI: 10.1155/2016/8393648.

[15] Meneghetti, P.; Qutubuddin, S., Synthesis, thermal properties and applications of polymer-clay nanocomposites. *Thermochim. Acta.* **2006**, *442*, 74-77, DOI: 10.1016/j.tca.2006.01.017.

[16] Che Ramli, Z. A., Photocatalytic degradation of methylene blue under UV light irradiation on prepared carbonaceous. *Sci. World J.* **2014**, DOI: 10.1155/2014/415136.

[17] Hao, P.; Ma, X.; Xie, J.; Lei, F.; Li, L.; Zhu, W.; Cheng, X.; Cui, G.; Tang, B., Removal of toxic metal ions using chitosan coated carbon nanotube composites for supercapacitors. *Sci. China Chem.* **2018**, *61*, 797-805. DOI: 10.1007/s11426-017-8215-7.

[18] Ghasemian Lemraski, E.; Sharafinia, S.; Alimohammadi, M., New activated carbon from Persian mesquite grain as an excellent adsorbent. *Phys. Chem. Res.* **2017**, *5*, 81-98, DOI:

10.22036/pcr.2017.38495.

[19] Verma, R.; Gangwar, J.; Srivastava, A. K., Multiphase TiO_2 nanostructures: A review of efficient synthesis, growth mechanism, probing capabilities, and applications in bio-safety and health. *RSC Adv.* **2017**. *7*, 44199-224, DOI: 10.1039/C7RA06925A.

[20] Verma, R.; Awasthi, A.; Singh, P.; Srivastava, R.; Sheng, H.; Wen, J., Interactions of titania based nanoparticles with silica and green-tea: Photo-degradation and-luminescence. *J. Colloid Interface Sci.* **2016**, *475*, 82-95, DIO: 10.1016/ j.jcis.2016.04.038.

[21] Das, J.; Freitas, F. S.; Evans, I. R.; Nogueira, A. F.; Khushalani, D., A facile nonaqueous route for fabricating titania nanorods and their viability in quasi-solid-state dye-sensitized solar cells. *J. Mater. Chem*. **2010**, *20*, 4425-31, DOI: 10.1039/B921373B.

[22] Silva, F.; Dore, C.; Marques, C.; Nascimento, M.; Benevides, N.; Rocha, H., Anticoagulant activity, paw edema and pleurisy induced carrageenan: Action of major types of commercial carrageenans. Carbohydr. Polym. **2010**, 79, 26-33, DOI: 10.1016/j.carbpol.2009.07.010.

[23] Wolkers, W. F.; Oliver, A. E.; Tablin, F.; Crowe, J. H., A Fourier-transform infrared spectroscopy study of sugar glasses. *Carbohydr. Res.* **2004**, *339*, 1077-85, DOI: 10.1016/j.carres.2004.01.016.

[24] Melo-Silveira, R. F.; Fidelis, G. P.; Costa, M. S. S. P.; Telles, C. B. S.; Dantas-Santos, N.; Elias, S. D. O., *In vitro* antioxidant, anticoagulant and antimicrobial activity and in inhibition of cancer cell proliferation by xylan extracted from corn cobs. *Int. J. Mol. Sci.* **2012**, *13*, 409-26, DOI: 10.3390/ ijms13010409.

[25] Vino, A. B.; Ramasamy, P.; Shanmugam, V.; Shanmugam, A., Extraction, characterization and in vitro antioxidative potential of chitosan and sulfated chitosan from Cuttlebone of Sepia aculeata Orbigny. *Asian Pac. J. Trop. Biomed.* **2012**, *2*, S334-S41, DOI: 10.1016/S2221-1691(12)60184-1.

[26] Song, C.; Yu, H.; Zhang, M.; Yang, Y.; Zhang, G., Physicochemical properties and antioxidant activity of chitosan from the blowfly Chrysomya megacephala larvae. *Int. J. Biol. Macromol.* **2013**, *60*, 347-54, DOI: 10.1016/j.ijbiomac.2013.05.039.

[27] Sahu, M. K.; Patel, R. K., Removal of safranin-O dye from aqueous solution using modified red mud: kinetics and equilibrium studies. *RSC Adv.* **2015**, *5*, 78491-501, DOI: 10.1039/C5RA15780C.

[28] Li, Y., Photocatalytic degradation of methyl orange by TiO_2-coated activated carbon and kinetic study. *Water Res.* **2006**, *40*, 1119-1126, DOI: 10.1016/ j.watres.2005.12.042.

[29] Lemraski, E. G.; Palizban, Z., Comparison of 2-amino benzyl alcohol adsorption onto activated carbon, silicon carbide nanoparticle and silicon carbide nanoparticle loaded on activated carbon. *J. Mol. Liq.* **2015**, *212*, 245-258, DOI: 10.1016/ j.molliq.2015.09.007.

[30] Baniamerian, H.; Safavi, M.; Alvarado-Morales, M.; Tsapekos, P.; Angelidaki, I.; Shokrollahzadeh, S., Photocatalytic inactivation of Vibrio fischeri using Fe_2O_3-TiO_2-based nanoparticles. *Environ. Res.* **2018**, *166*, 497-506, DOI: 10.1016/j.envres.2018.06.011.

[31] Ganesh, I.; Kumar, P. P.; Gupta, A. K.; Sekhar, P. S.; Radha, K.; Padmanabham, G.; Sundararajan, G., Preparation and characterization of Fe-doped TiO_2 powders for solar light response and photocatalytic applications. *Process. Appl. Ceram.* **2012**, *6*, 21-36, DOI: 10.2298/PAC1201021G.

[32] Hu, Y.; Wang, H.; Yang, L.; Liu, X.; Zhang, B.; Liu, Y.; Fu, H., Preparation of chitosan-based activated carbon and its electrochemical performance for EDLC. *J. Electrochem. Soc.* **2013**, *160*, H321. DOI: 10.1149/2.062306jes.

[33] Kannan, N.; Sundaram, M. M., Kinetics and mechanism of removal of methylene blue by adsorption on various carbons-a comparative study. *Dyes Pigm.* **2001**, *51*, 25-40, DOI: 10.1016/S0143-7208(01)00056-0.

[34] Zainal, Z., Characterization of TiO_2-chitosan/glass photocatalyst for the removal of a monoazo dye *via* photodegradation-adsorption process. *J. Hazard. Mater.* **2009**, *164*, 138-145, DOI: 10.1016/ j.jhazmat.2008.07.154.

[35] Chen, S., Equilibrium and kinetic studies of methyl orange and methyl violet adsorption on activated carbon derived from Phragmites australis.

Desalination. **2010**, *252*, 149-156, DOI: 10.1016/j.desal.2009.10.010.

[36] Vargas, A. M., NaOH-activated carbon from flamboyant (Delonix regia) pods: Optimization of preparation conditions using central composite rotatable design. *Chem. Eng. J.* **2010**, *162*, 43-50, DOI: 10.1016/j.cej.2010.04.052.

[37] Gao, H.; Zhao, S.; Cheng, X.; Wang, X.; Zheng, L., Removal of anionic azo dyes from aqueous solution using magnetic polymer multi-wall carbon nanotube nanocomposite as adsorbent. *Chem. Eng. Technol.,* **2013**, *223*, 84-90. DOI: 10.1016/j.cej.2013.03.004.

[38] Chandane, V.; Singh, V., Adsorption of safranin dye from aqueous solutions using a low-cost agro-waste material soybean hull. *Desalin Water Treat.* **2016**, *57*. 4122-4134, DOI: 10.1080/ 19443994.2014.991758.

[39] Chandane, V.; Singh, V., Adsorption of safranin dye from aqueous solutions using a low-cost agro-waste material soybean hull. *Desalin. Water Treat.* **2016**, *57*. 4122-4134. DOI: org/ 10.1080/19443994.2014.991758

[40] Chen, S.; Zhang, J.; Zhang, C.; Yue, Q.; Li, Y.; Li, C., Equilibrium and kinetics studies of methyl orange and methyl violet adsorption on activated carbon derived from phragmites australis. *Desalination*. **2010**, *252*, 149-156, DOI: 10.1016/ j.desal.2009.10.010.

[41] Noorimotlagh, Z., Adsorption of textile dye in activated carbons prepared from DVD and CD wastes modified with multi-wall carbon nanotubes: Equilibrium isotherms, kinetics and thermodynamic study. *Chem. Eng. Res. Des.* **2019**, *141*, 290-301, DOI: 10.1016/j.cherd.2018.11.007.

[42] Yang, J.; Yu, M.; Chen, W., Adsorption of hexavalent chromium from aqueous solution by activated carbon prepared from longan seed: Kinetics, equilibrium and thermodynamics. *J. Ind. Eng. Chem.* **2015**, *21*, 414-422, DOI: 10.1016/ j.jiec.2014.02.054.

[43] Langmuir, I., The constitution and fundamental properties of solids and liquids. *Part I. Solids. Acs.* **1916**, *38*, 2221-2295, DOI: 10.1021/ja02268a002.

[44] Freundlich, H., Über die adsorption in lösungen. *Z Phys. Chem.* **1907**, *57*, 385-470.

[45] Temkin, M.; Pyzhev, V., Recent Modifications to Langmuir Isotherms. **1940**.

[46] Dada, A., Langmuir, Freundlich, Temkin and Dubinin-Radushkevich isotherms studies of equilibrium sorption of Zn^{2+} unto phosphoric acid modified rice husk. *IOSR J. Appl. Chem.* **2012**. *3*, 38-45, DOI: 10.9734/JPRI/2017/38056.

[47] Lagergren, S., Zur Theorie der Sogenannten Adsorption Geloster Stoffe. **1898**.

[48] Ho, Y. -S.; McKay, G., Pseudo-second order model for sorption processes. *Process. Biochem.* **1999**, *34*, 451-465, DOI: 10.1016/S0032-9592(98)00112-5.

[49] Elovich, S. Y.; Larionov, O., Theory of adsorption from nonelectrolyte solutions on solid adsorbents. *Bull. Acad. Sci. USSR, Div. Chem. Sci.* **1962**, *11*, 191-197.

[50] Safarik, I.; Safarikova, M., Magnetic fluid modified peanut husks as an adsorbent for organic dyes removal. *Phys. Procedia*. **2010**, *9*, 274-278, DOI: 10.1016/j.phpro.2010.11.061.

[51] Safarikoval, M., Dye adsorption on magnetically modified Chlorella vulgaris cells. *Fresenius Environ. Bull.* **2008**, *17*, 486-492, http://hdl.handle.net/10400.14/2778.

[52] Angelova, R., Magnetically modified Sargassum horneri biomass as an adsorbent for organic dye removal. *J. Clean. Prod.* **2016**, *137*, 189-194, DOI: 10.1016/j.jclepro.2016.07.068.

[53] Malekbala, M. R., The study of the potential capability of sugar beet pulp on the removal efficiency of two cationic dyes. *Chem. Eng. Sci.* **2012**, *90*, 704-712, DOI: 10.1016/ j.cherd.2011.09.010.

[54] El Haddad, M., Evaluation of potential capability of calcined bones on the biosorption removal efficiency of safranin as cationic dye from aqueous solutions. *J. Taiwan Inst. Chem. Eng.* **2013**, *44*, 13-18, DOI: 10.1016/j.jtice.2012.10.003.

[55] Safarik, I., *et al.,* Magnetically modified spent coffee grounds for dyes removal. *Eur. Food Res. Technol.* **2012**, *234*, 345-350, DOI: 10.1007/s00217-011-1641-3.